PROCEEDINGS OF SCIENCE

Forward di-jets in p+A collisions in the ITMD framework

Marek Matas*
Faculty of Nuclear Sciences and Physical Engineering, Czech Technical University in Prague, Czech Republic
E-mail: matas.marek1@gmail.com

Cyrille Marquet
CPHT, École Polytechnique, CNRS, Université Paris-Saclay, F-91128 Palaiseau, France
E-mail: cyrille.marquet@polytechnique.edu

Within the Color Glass Condensate (CGC) framework, we compute the cross section for di-jet events in the forward rapidity region in p+p and p+Pb collisions at the LHC. We make use of the recently proposed improved transverse-momentum-dependent (ITMD) factorization formula for forward di-jets, derived from CGC expressions when the jet momenta are much bigger than the saturation scale. This process is nevertheless sensitive to effects of non-linear QCD evolution, when the total transverse momentum of the jet pair is small, and as a direct consequence of those saturation effects, we predict a suppression of the nuclear modification factor for back-to-back jets. We obtain $R_{pPb} \sim 0.5$ for central collisions, and argue that the measurement of the azimuthal angle dependence of the nuclear modifications of forward di-jet events could provide a strong evidence for gluon saturation.

XXVI International Workshop on Deep-Inelastic Scattering and Related Subjects (DIS2018)
16-20 April 2018
Kobe, Japan

*Speaker.

PoS(DIS2018)055

1. Introduction

Forward-rapidity measurements in high-energy p+p and p+A collisions are sensitive to the low-x properties of the wave function of protons and nuclei. They single out dilute-dense collisions which may provide access to the non-linear regime of parton saturation in QCD. The onset of this regime is characterized by the saturation momentum Q_s, which for heavy-ion targets scales with the mass number A as $A^{\frac{1}{6}}$.

There has been some evidence in the RHIC data on forward di-hadron production at low p_t, to support the existence of such non-linear regime [1, 2, 3, 4]; in this work we shall address the presence of these effects in forward di-jet events at the LHC. To compute the forward di-jet cross section, we shall use an approximation of Color Glass Condensate (CGC) expressions that involves transverse-momentum-dependent (TMD) gluon distributions. This approximation, valid in the presence of a hard scale, was dubbed improved TMD (ITMD) factorization.

2. The specificity of forward back-to-back di-jets

The detection of saturation effects in data has proven to be difficult, due to the fact that the low-x gluons with transverse momentum k_t of the order of Q_s are often accessible only in a small corner of the kinematical window at colliders, when concurrently one would like those scales to be large enough to justify the use of weak-coupling calculations.

The forward di-jet process is particularly interesting as it features hard scales $|\vec{p_1}_t|, |\vec{p_2}_t| \gg Q_s$ (where $\vec{p_1}_t$ and $\vec{p_2}_t$ are the transverse momenta of the two outgoing jets) while still being sensitive to low gluon k_t, of the order of Q_s. This happens when the two jets are back-to-back in the transverse plane (and with $|\vec{p}_t|$'s of the same magnitude): their transverse momenta cancel out and the total transverse momentum of the pair

$$k_t = |\vec{p_1}_t + \vec{p_2}_t| = \left(\vec{p_1}_t{}^2 + \vec{p_2}_t{}^2 + 2|\vec{p_1}_t||\vec{p_2}_t|\ \cos\Delta\Phi\right)^{1/2} \tag{2.1}$$

gets small for $\Delta\Phi \simeq \pi$.

Furthermore, we want to select events in which x_1 is large (partons from the projectile proton) and x_2 is low (gluons from the target proton or nucleus). The condition of $x_2 \ll 1$ is necessary in order to probe saturation effects in the target, while large values of x_1 are required in order to neglect the partonic transverse momentum on the projectile side and describe it in terms of parton distribution functions that are known with great precision from previous experiments. Since

$$x_1 = \frac{1}{\sqrt{s}}\left(|\vec{p_1}_t|\, e^{y_1} + |\vec{p_2}_t|\, e^{y_2}\right) \quad \text{and} \quad x_2 = \frac{1}{\sqrt{s}}\left(|\vec{p_1}_t|\, e^{-y_1} + |\vec{p_2}_t|\, e^{-y_2}\right)$$

where $\sqrt{s}$ denotes the CMS energy of the collision and y_1 and y_2 are the rapidities of the two jets, we can achieve both conditions by imposing y_1 and y_2 to be large (in our case between 3.5 and 4.5).

3. The ITMD factorized cross section

The cross section for the considered process can be expressed as [5]

$$\frac{d\sigma^{pA\to j_1+j_2+X}}{d^2P_t d^2k_t dy_1 dy_2} = \frac{\alpha_s^2}{(x_1x_2s)^2}\sum_{a,c,d} x_1 f_{a/p}(x_1)\sum_i \frac{1}{1+\delta_{cd}} K^{(i)}_{ag*\to cd}(P_t,k_t)\Phi^{(i)}_{ag}(x_2,k_t), \tag{3.1}$$

where δ_{cd} is the Kronecker delta, α_s is the QCD coupling, and P_t is the hard momentum scale of the process, related to $|\vec{p_{1t}}|$ and $|\vec{p_{2t}}|$. The functions $x_1 f_{a/p}(x_1)$ are collinear parton distribution function for the projectile, the factors $K^{(i)}_{ag*\to cd}(P_t,k_t)$ are the 2-to-2 matrix elements with non-zero k_t computed in [5] for the three channels $qg^* \to qg$, $gg^* \to q\bar{q}$ and $gg^* \to gg$, while the distributions $\Phi^{(i)}_{ag}(x_2,k_t)$ are the TMD gluon distributions that carry the information about the non-linear QCD dynamics of the small-x_2 target. This will be discussed in more details in the following sections.

Formula (3.1) interpolates between two limiting cases both contained in the CGC framework, while bypassing the full complexity of the CGC expressions. Those are (i) the high-energy factorization (HEF) limit, $P_t\,,\ k_t \gg Q_s$, formaly obtained from (3.1) when all the gluon TMDs $\Phi^{(i)}_{ag}$ coincide, and valid for $\Delta\Phi$ away from π when only linear small-x effects matter [6, 7], and (ii) the TMD limit, $P_t \gg k_t\,,\ Q_s$, formaly obtained when $K^{(i)}(P_t,k_t) \to K^{(i)}(P_t,0)$ and valid for nearly back-to-back jets; this is when saturation effects are the largest [8, 9].

4. The dipole scattering amplitude and the BK equation

In order to compute the gluon TMDs, we shall utilize the Balitsky-Kovchegov (BK) evolution equation [10, 11]. In this work we assume that the impact parameter dependence (denoted as b) of the scattering amplitude N (which is the solution of the BK equation) factorizes and the integral over the impact parameter can be replaced with a constant factor due to its independence of the evolution. The BK equation with running coupling corrections (rcBK equation), reads

$$\frac{\partial N(r,x)}{\partial \ln(x_0/x)} = \int d^2\mathbf{r_1}\, K^{\mathrm{run}}(\mathbf{r},\mathbf{r_1},\mathbf{r_2})\,[N(r_1,x)+N(r_2,x)-N(r,x) \\ -N(r_1,x)N(r_2,x)]\ , \tag{4.1}$$

with $\mathbf{r_2} \equiv \mathbf{r}-\mathbf{r_1}$, and where x_0 is some initial value for the evolution. K^{run} is the evolution kernel including running coupling corrections [12]:

$$K^{\mathrm{run}}(\mathbf{r},\mathbf{r_1},\mathbf{r_2}) = \frac{N_c\,\alpha_s(r^2)}{2\pi^2}\left[\frac{1}{r_1^2}\left(\frac{\alpha_s(r_1^2)}{\alpha_s(r_2^2)}-1\right)+\frac{r^2}{r_1^2\,r_2^2}+\frac{1}{r_2^2}\left(\frac{\alpha_s(r_2^2)}{\alpha_s(r_1^2)}-1\right)\right]. \tag{4.2}$$

The rcBK evolution is independent of whether the target is a proton or a nucleus, which is accounted for in the initial condition. We use the McLerran-Venugopalan (MV) intial condition:

$$N(r,x{=}x_0) = 1-\exp\left[-\frac{r^2\,Q_{s0}^2}{4}\,\ln\left(\frac{1}{\Lambda r}+e\right)\right]\ , \tag{4.3}$$

with $\Lambda = 0.241$ GeV where Q_{s0} denotes the saturation scale at the initial value x_0 (we use $x_0 = 0.01$). The value of the saturation scale for protons was obtained from a fit to deep-inelastic scattering data as $Q^2_{s0}(p) = 0.2\,\mathrm{GeV}^2$ [13]. For nuclei, this value was obtained from a fit to single-hadron minimum-bias d+Au data at RHIC [14]. The fit resulted in the value of $0.4\,\mathrm{GeV}^2$ and to obtain the saturation scale for central collisions for nuclei, we make use of the Woods-Saxon distribution which predicts an increase of about 1.5 with respect to the minimum-bias events. The value we shall use when considering central p+A collisions is then $Q^2_{s0}(Pb)$=$0.6\,\mathrm{GeV}^2$.

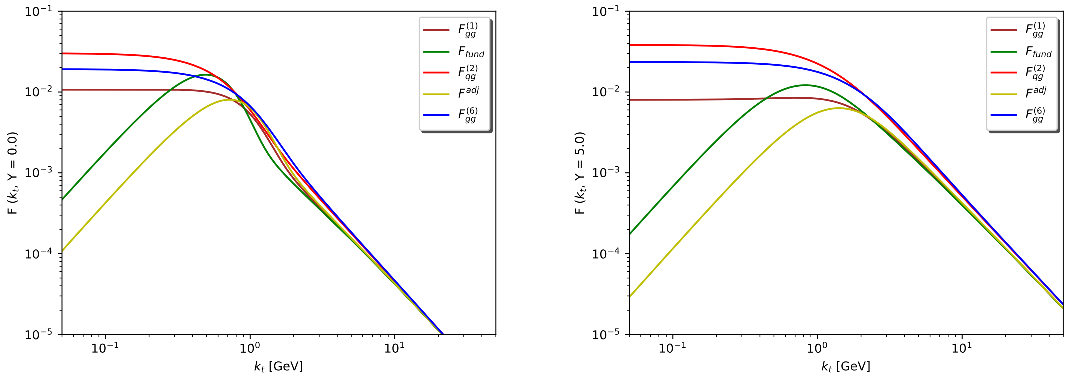

Figure 1: The various gluon TMDs that contribute to the forward di-jet process, shown for the initial condition at $Y = \ln(x_0/x_2) = 0$ (left) and after some rcBK evolution for $Y = 5$ (right). The shown TMDs do not include the common factor $S_\perp/\alpha_s$.

5. The rcBK gluon TMDs

The TMDs that describe the target and carry the information about the saturation effects can be calculated with the use of the impact parameter independent rcBK equation. Using the Gaussian approximation of the CGC along with the large-N_c limit, we follow the steps outlined in [15], where a different implementation of the BK evolution was studied.

We can use the scattering amplitude $N(x,\mathbf{r})$, which is the solution of the Balitsky-Kovchegov evolution equation, to calculate three gluon TMDs, the Weiszacker-Williams gluon distribution $\mathscr{F}_{WW}$, the fundamental dipole gluon distribution $\mathscr{F}_{fund}$ and the adjoint dipole gluon distribution $\mathscr{F}_{adj}$:

$$\mathscr{F}_{WW}(x_2,k_t) = \frac{C_F\, S_\perp}{2\alpha_s\pi^4}\int d^2b \int \frac{d^2\mathbf{r}}{\mathbf{r}^2}\, e^{-ik_t\cdot\mathbf{r}}\, \left\{1-[1-N(x_2,\mathbf{r})]^2\right\} , \tag{5.1}$$

$$\mathscr{F}_{fund}(x_2,k_t) = \frac{N_c\, k_t^2\, S_\perp}{2\pi^2\alpha_s}\int \frac{d^2\mathbf{r}}{(2\pi)^2} e^{-ik_t\cdot\mathbf{r}}[1-N(x_2,\mathbf{r})] \equiv \frac{N_c\, k_t^2\, S_\perp}{2\pi^2\alpha_s}\, F(x_2,k_t), \tag{5.2}$$

$$\mathscr{F}_{adj}(x_2,k_t) = \frac{C_F\, k_t^2\, S_\perp}{2\pi^2\alpha_s}\int \frac{d^2\mathbf{r}}{(2\pi)^2} e^{-ik_t\cdot\mathbf{r}}[1-N(x_2,\mathbf{r})]^2 . \tag{5.3}$$

where $S_\perp$ is a constant, that represents the transverse size of target.

In the notations of [15], $\mathscr{F}_{WW} = x_2 G^{(1)}$, $\mathscr{F}_{fund} = x_2 G^{(2)}$, and $\mathscr{F}_{adj} = \mathscr{F}_{gg}^{(1)} - \mathscr{F}_{gg}^{(2)}$ (see [4]). Three additional gluon TMDs are needed in the computation of the di-jet cross section (3.1), and are obtained via the following convolutions:

$$\mathscr{F}_{qg}^{(2)}(x_2,k_t) = \int d^2q_t\, \mathscr{F}_{WW}(x_2,q_t) F(x_2,k_t-q_t), \tag{5.4}$$

$$\mathscr{F}_{gg}^{(1)}(x_2,k_t) = \int d^2q_t\, \mathscr{F}_{fund}(x_2,q_t) F(x_2,k_t-q_t), \tag{5.5}$$

$$\mathscr{F}_{gg}^{(6)}(x_2,k_t) = \int d^2q_t d^2q_t'\, \mathscr{F}_{WW}(x_2,q_t) F(x_2,q_t') F(x_2,k_t-q_t-q_t') . \tag{5.6}$$

The resulting TMDs are shown in Fig. 1, from which the $\Phi_{ag}^{(i)}$'s are easily obtained [5].

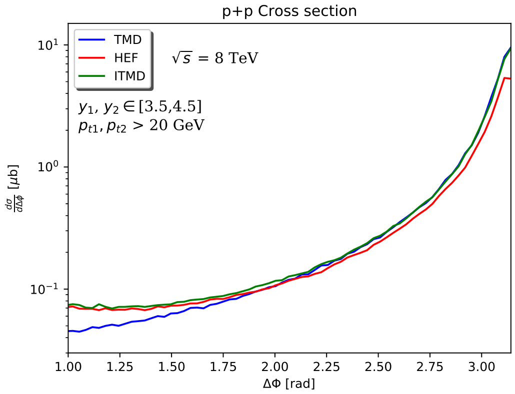

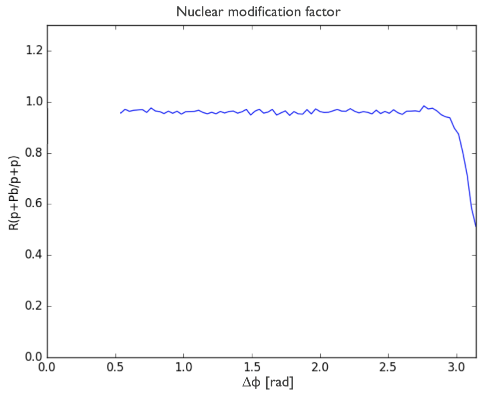

Figure 2: Left: cross section for forward di-jet events in p+p collisions at $\sqrt{s}$=8 TeV in the ITMD approach, as a function of the azimuthal angle between the jets $\Delta\Phi$, for $3.5 < y_1\,,\ y_2 < 4.5$ and $|p_{t1}|\,,\ |p_{t2}| > 20$ GeV. The curve is compared with the HEF and TMD limiting bevaviors. Right: nuclear modification factor in p+Pb collisions, showing large saturation effects near $\Delta\Phi = \pi$.

6. Cross section results and nuclear modification factor

The final cross section for di-jet events computed in this formalism is shown in Fig. 2-left as a function of the angle $\Delta\Phi$ between the two jets in the plane transverse to the collision axis. The sum of the jet-momenta gives the total transverse momentum k_t (see (2.1)), so low-values of $\Delta\Phi$ correspond to high k_t and vice versa. If we take a look at the cross section computed in the ITMD framework compared with the TMD and HEF approches, we can see that it reproduces the behavior of HEF in the high-k_t region and the behavior of TMD in the low-k_t region, as expected since those are their respective regions of validity. The ITMD framework is valid for both low and high regions of k_t, although the interesting regime in view of saturation effects is the low k_t one, for $\Delta\Phi \simeq \pi$.

In order to better reveal the presence of saturation effects, we shall exploit the fact the saturation scale is bigger in nuclei than in nucleons, and study the nuclear modification factor

$$R_{pPb} = \frac{d\sigma^{p+Pb}/d\Delta\Phi}{A\ d\sigma^{p+p}/d\Delta\Phi}\,. \tag{6.1}$$

We expect to observe a suppression when saturation effects become important because there will be less partons per nucleon available for the interaction in the lead nucleus than there is in a proton. This is indeed what happens, as is shown in Fig. 2-right, for central p+Pb collisions.

7. Conclusions

In this work, we have computed the nuclear modification factor for dilute-dense events with di-jets in the forward region in rapidity, in order to probe saturation effects. We have used the ITMD framework and obtained the gluon TMDs from the rcBK evolution equation.

We observe that R_{pPb} is suppressed when the two forward jets are emitted back-to-back, which is a signature of saturation effects, since in that region the total transverse momentum of the jet pair is comparable to the saturation scale of the lead nucleus: $k_t \sim Q_s(Pb)$.

Acknowledgments

The work of CM was supported in part by the Agence Nationale de la Recherche under the project ANR-16-CE31-0019-02. The work of MM has been supported by the grant 17-04505S of the Czech Science Foundation (GACR) and has been performed in the framework of COST Action CA15213 THOR. Computational resources were provided by the CESNET LM2015042 and the CERIT Scientific Cloud LM2015085, provided under the program "Projects of Large Research, Development, and Innovations Infrastructures".

References

[1] Javier L. Albacete and Cyrille Marquet. Azimuthal correlations of forward di-hadrons in d+Au collisions at RHIC in the Color Glass Condensate. *Phys. Rev. Lett.*, 105:162301, 2010.

[2] Anna Stasto, Bo-Wen Xiao, and Feng Yuan. Back-to-Back Correlations of Di-hadrons in dAu Collisions at RHIC. *Phys. Lett.*, B716:430–434, 2012.

[3] T. Lappi and H. Mantysaari. Forward dihadron correlations in deuteron-gold collisions with the Gaussian approximation of JIMWLK. *Nucl. Phys.*, A908:51–72, 2013.

[4] Javier L. Albacete, Giuliano Giacalone, Cyrille Marquet, and Marek Matas. Forward di-hadron back-to-back correlations in *pA* collisions from rcBK evolution. 2018.

[5] P. Kotko, K. Kutak, C. Marquet, E. Petreska, S. Sapeta, and A. van Hameren. Improved TMD factorization for forward dijet production in dilute-dense hadronic collisions. *JHEP*, 09:106, 2015.

[6] S. Catani, M. Ciafaloni, and F. Hautmann. High-energy factorization and small x heavy flavor production. *Nucl. Phys.*, B366:135–188, 1991.

[7] M. Deak, F. Hautmann, H. Jung, and K. Kutak. Forward Jet Production at the Large Hadron Collider. *JHEP*, 09:121, 2009.

[8] Fabio Dominguez, Cyrille Marquet, Bo-Wen Xiao, and Feng Yuan. Universality of Unintegrated Gluon Distributions at small x. *Phys. Rev.*, D83:105005, 2011.

[9] C. Marquet, E. Petreska, and C. Roiesnel. Transverse-momentum-dependent gluon distributions from JIMWLK evolution. *JHEP*, 10:065, 2016.

[10] I. Balitsky. Operator expansion for high-energy scattering. *Nucl. Phys.*, B463:99–160, 1996.

[11] Yuri V. Kovchegov. Small x F(2) structure function of a nucleus including multiple pomeron exchanges. *Phys. Rev.*, D60:034008, 1999.

[12] Ian Balitsky. Quark contribution to the small-x evolution of color dipole. *Phys. Rev.*, D75:014001, 2007.

[13] Javier L. Albacete, Nestor Armesto, Jose Guilherme Milhano, Paloma Quiroga-Arias, and Carlos A. Salgado. AAMQS: A non-linear QCD analysis of new HERA data at small-x including heavy quarks. *Eur. Phys. J.*, C71:1705, 2011.

[14] Javier L. Albacete and Cyrille Marquet. Single Inclusive Hadron Production at RHIC and the LHC from the Color Glass Condensate. *Phys. Lett.*, B687:174–179, 2010.

[15] A. van Hameren, P. Kotko, K. Kutak, C. Marquet, E. Petreska, and S. Sapeta. Forward di-jet production in p+Pb collisions in the small-x improved TMD factorization framework. *JHEP*, 12:034, 2016.